SPUTTERED THIN FILM RESEARCH

Alexander J. Shuskus, et al

United Aircraft Research Laboratories

Prepared for:

Office of Naval Research
Advanced Research Projects Agency

27 May 1973

SPUTTERED THIN FILM RESEARCH

Second Semi-Annual Technical Report

PERIOD COVERED: 16 OCTOBER 1972 TO 15 APRIL 1973

MAY 29, 1973

PREPARED UNDER CONTRACT N00014-72-C-0415

Sponsored By

Advanced Research Projects Agency
ARPA Order No. 2173, Amendment No. 1
Monitored By Office of Naval Research

United Aircraft
Research Laboratories

UNITED AIRCRAFT CORPORATION

EAST HARTFORD, CONNECTICUT 06108

DISCLAIMER NOTICE

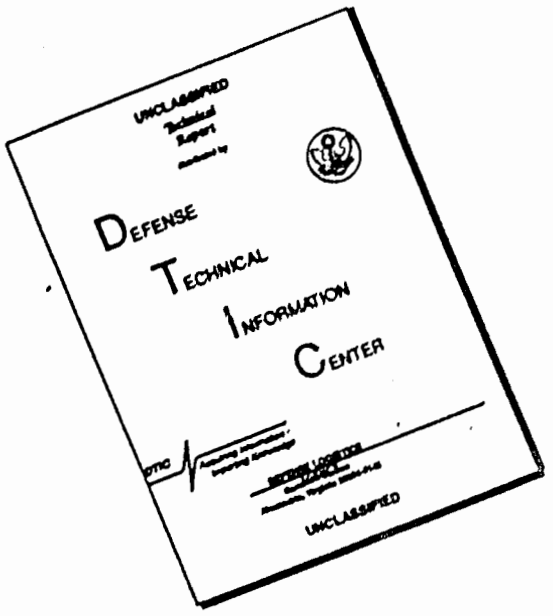

THIS DOCUMENT IS BEST QUALITY AVAILABLE. THE COPY FURNISHED TO DTIC CONTAINED A SIGNIFICANT NUMBER OF PAGES WHICH DO NOT REPRODUCE LEGIBLY.

Unclassified
Security Classification

DOCUMENT CONTROL DATA - R & D

(Security classification of title, body of abstract and indexing annotation must be entered when the overall report is classified)

1 ORIGINATING ACTIVITY (Corporate author) United Aircraft Corporation Research Laboratories East Hartford, Connecticut 06103	2a. REPORT SECURITY CLASSIFICATION Unclassified 2b. GROUP

3 REPORT TITLE

Sputtered Thin Film Research

4 DESCRIPTIVE NOTES (Type of report and inclusive dates)

Semi-Annual Report for the Period 16 October 1972 to 15 April 1973

5 AUTHOR(S) (First name, middle initial, last name)

A. J. Shuskus, Daniel J. Quinn, Edouard L. Paradis, James M. Berak, Thomas M. Reeder

6 REPORT DATE May 27, 1973	7a. TOTAL NO. OF PAGES 68	7b. NO OF REFS 13
8a. CONTRACT OR GRANT NO N00014-72-C-0415 b. PROJECT NO c. ARPA Order No. 2173, Amendment No. 1 d.	9a. ORIGINATOR'S REPORT NUMBER(S) M951337-6 9b. OTHER REPORT NO(S) (Any other numbers that may be assigned this report)	

10 DISTRIBUTION STATEMENT

11 SUPPLEMENTARY NOTES	12 SPONSORING MILITARY ACTIVITY Department of the Navy Office of Naval Research

13 ABSTRACT

Current progress toward establishing the feasibility of reactive rf sputtering as a means of preparing single crystal films suitable for integrated optics and electronics applications is discussed. Single crystal films of aluminum nitride, zinc oxide, rutile and gallium arsenide have been successfully grown by this technique. Epitaxy of aluminum nitride and zinc oxide has been obtained on (0001) and ($1\bar{1}02$) sapphire substrates, rutile on ($1\bar{1}02$) sapphire and gallium arsenide on semi-insulating substrates of gallium arsenide.

Surface acoustic wave delay lines were fabricated to evaluate the piezoelectric qualities of the zinc oxide and aluminum nitride films. The piezoelectric coupling coefficients determined indicate that the quality of the sputtered films is comparable to the best results reported for films prepared by chemical vapor deposition.

DD FORM 1 NOV 68 1473

Unclassified
Security Classification

14. KEY WORDS	LINK A		LINK B		LINK C	
	ROLE	WT	ROLE	WT	ROLE	WT
Thin Films						
Reactive Sputtering						
Single Crystal						
Aluminum Nitride						
Zinc Oxide						
Rutile						
Gallium Arsenide						
Surface Acoustic Wave						
Epitaxy						

UNITED AIRCRAFT COPRORATION
RESEARCH LABORATORIES
East Hartford, Connecticut

M951337-6

Second Semi-Annual Report Under Contract N00014-72-C-0415
16 October 1972 to 15 April 1973

ARPA Order No.:	2173, Amendment No. 1
Program Cost Code:	000003D10K21
Contractor:	United Aircraft Research Laboratories
Effective Date of Contract:	15 April 1972
Contract Expiration Date:	30 September 1973
Amount of Contract:	$273,707.00
Contract Number:	N00014-72-C-0415
Contract Management:	Dr. Anthony J. DeMaria (203)565-3545
Principal Investigator:	Dr. Alexander J. Shuskus (203)565-6498
Scientific Officer:	Dr. F. B. Isakson
Short Title:	Sputtered Thin Film Optics
Reported By:	A. J. Shuskus, D. J. Quinn, E. L. Paradis J. M. Berak, T. M. Reeder

Sponsored by Advanced Research Projects Agency
ARPA Order No. 2173, Amendment No. 1

Report M951337-6

Interim Technical Report Under Contract N00014-72-C-0415
for the Period 16 October 1972 through 15 April 1973

Sputtered Thin Film Research

ARPA Order No. 2173, Amendment No. 1, Project Code No. 3D10

TABLE OF CONTENTS

TABLE OF CONTENTS
(cont'd)

LIST OF ILLUSTRATIONS

1.0 SUMMARY

1.1 Program Objective

The major objective of the program is to establish the feasibility of reactive rf sputtering as a viable approach for the preparation of single crystal thin films suitable for applications in microelectronics, microwave devices and integrated optics. It involves the preparation of epitaxial films of selected III-V semiconductors, II-VI semiconductors and high dielectric constant materials. A secondary objective of the program is fabrication of appropriate devices to ascertain the device potential of the films grown. This research program is being conducted under the ARPA/ONR Contract N00014-72-C-0415.

1.2 Major Accomplishments

Over the last six month period considerable progress has been achieved. Conditions for the epitaxial growth of four different materials have been established. Each accomplishment in itself constitutes a first.

Single crystal films of aluminum nitride have been grown by reactive sputtering in a nitrogen and ammonia ambient on (0001) and ($1\bar{1}02$) oriented sapphire substrates. Surface acoustic wave devices were fabricated and the results obtained were comparable to the best reported for AlN on sapphire grown by chemical vapor deposition. The results are extremely encouraging in that process development for the growth of aluminum nitride by reactive sputtering is in its infancy as compared to the chemical vapor deposition process which has had several years to mature. The films prepared have a surface finish superior to that obtained by chemical vapor deposition.

Single crystal films of zinc oxide have been grown on (0001) and ($1\bar{1}02$) oriented sapphire substrates. The preparation of epitaxial single crystal films of zinc oxide by sputtering on ($1\bar{1}02$) oriented sapphire has not been previously reported in the literature. Epitaxy has been achieved at a deposition rate approaching two orders of magnitude improvement over past work reported on zinc oxide grown by sputtering on (0001) sapphire. The improvement achieved in deposition rate establishes sputtering as a practical method for preparation of single crystal films of zinc oxide.

Single crystal films of gallium arsenide have been prepared by reactive sputtering of gallium in an arsenic ambient. This is the first known successful attempt at epitaxy of gallium arsenide by reactive sputtering. The films initially grown have a resistivity of 10^4 Ω-cm.

The conditions for the growth of epitaxial films of rutile on sapphire were also determined. These results constitute the first successful preparation of single crystal rutile films by reactive sputtering.

The results achieved to date clearly illustrate the versatility and feasibility of reactive sputtering as a viable approach to the preparation of a wide variety of materials in single crystal thin film form. Surface quality and film uniformity achieved by sputtering is generally superior to that obtained by chemical vapor deposition.

1.3 Future Work

The bulk of the effort to date has been directed toward establishing conditions for epitaxial growth and the structural characterization of the film. In order to consolidate the gains of the past period most of the effort will be focused on the materials grown to date. Greater attention will be given to the fabrication and evaluation of a number of device configurations. The results obtained will be used to further refine the deposition parameters in order to achieve the optimum material properties. Experiments in optical waveguiding will be carried out. Active thin film devices incorporating acoustooptic interactions will be fabricated with single crystal aluminum nitride and zinc oxide films. Doping experiments will be conducted on the reactively sputtered gallium arsenide. Preliminary work will start on the epitaxial growth of reactively sputtered gallium nitride and aluminum arsenide.

2.0 EPITAXY OF ALUMINUM NITRIDE BY REACTIVE SPUTTERING

Single crystal films of aluminum nitride have been grown on (0001) and ($1\bar{1}02$) oriented sapphire substrates by reactive rf sputtering in both nitrogen and ammonia ambients. Although single crystal films of aluminum nitride have been prepared by chemical vapor deposition (Refs. 1, 2) we believe that this represents the first successful attempt to achieve this result via sputtering.

Aluminum nitride is a particularly interesting material for surface acoustic wave and integrated optics applications. Its crystal structure is hexagonal wurtzite with lattice parameters $a_o = 3.111\text{Å}$ and $c_o = 4.980\text{Å}$. It is piezoelectric and electrooptic.

The initial efforts of this program were directed toward establishing the feasibility of using the reactive rf sputtering technique for preparation of single crystal thin films, determination of the conditions for epitaxy and characterization of the films grown. The results obtained over the last six month period are described below.

2.1 Epitaxial Thin Film Deposition

In the previous report period the maximum substrate temperature attainable was limited to approximately 750°C. Epitaxy was not achieved and modification of the system was required to extend its high temperature capabilities. A tantalum substrate heater was incorporated into the system which permitted a substrate heater operating temperature in excess of 1800°C. The actual sample temperature was determined in the following manner. The substrate heater temperature was measured by an optical pyrometer and the actual sample temperature was arrived at by measuring its thermal expansion at the corresponding heater temperature. Plots were made of the substrate heater temperature versus sample temperature in order to convert the optical pyrometer readings directly into substrate temperature. More complete details of this measurement are discussed in Appendix I.

Substrates were polished single crystal aluminum oxide. Crystals cut with the (0001) plane parallel to the surface as well as crystals cut with the ($1\bar{1}02$) plane parallel to the surface were used. Substrates were prepared by a thorough degreasing in MOS grade trichloroethylene followed by a rinse in MOS grade methanol and finally a rinse in deionized water. The substrates were next slightly etched in 55°C H_2SO_4 for 15 minutes, rinsed in deionized water and dried in a dry nitrogen blast. Finally the substrates were annealed for 2 hours at 1200°C in dry oxygen.

The relative merits of ammonia and nitrogen were studied as the reactant gas. Although epitaxy could be achieved using either gas, ammonia was found to result in epitaxial deposits at a lower temperature. The films obtained with ammonia were

generally clear although films with a hazy appearance were produced on occasion. The elevated temperature (1400°C) required for epitaxial growth of AlN films in nitrogen resulted in an apparent reaction between the substrate and the substrate heater. This produced a blackening of the heater and the underside of the substrate. The resultant films generally had a rough surface texture. Due to this problem, subsequent work was done solely with an ammonia reactive ambient. Typical conditions for obtaining epitaxy of aluminum nitride on (0001) and ($1\bar{1}02$) sapphire substrates are listed below:

Reactive Ambient	- 2×10^{-2} torr NH_3
Substrate Temperature	- 1250°C
Deposition Rate	- 50 Å/min
Reactive Ambient	- 6×10^{-2} torr N_2
Heater Temperature	- 1400°C
Deposition Rate	- 20 Å/min

Epitaxy has been achieved at a substrate temperature as low as 1050°C with an ammonia ambient but the results are spotty. It is preferable to grow at the slightly higher temperature quoted in order to achieve consistent results.

Prior to film deposition a new tantalum heater is prepared for use in the following manner. The vacuum chamber is pumped down to 10^{-6} torr and the heater is rasied to 1200°C and outgassed till the background pressure drops back to 10^{-6} torr. Subsequently, the heater temperature is raised to 1800°C for five minutes and then dropped back to 1400°C, and a coating of aluminum nitride is deposited on the tantalum heater.

After a heater is broken in, a typical run sequence consists of (1) evacuating the sputtering chamber to 10^{-6} torr with the heater adjusted to operating temperature, (2) admission of the reactive gas into the chamber and adjustment to operating pressure (typically 2×10^{-2} torr), (3) readjustment of the heater to the required deposition temperature, and (4) sputter cleaning of the aluminum target for five minutes at a power density of 40 W/in^2. With the completion of this sequence the system is ready for film deposition. The sputtering target is 99.999% pure aluminum and the reactive gases have an assayed purity of 99.999% or better.

2.2 Physical Characterization of AlN Films

Reflection electron diffraction and x-ray diffraction were employed to determine the structure and epitaxial relationships of the film to the substrate. Figure 1 shows the calculated reflection electron diffraction pattern expected for the electron beam aligned with the [$10\bar{1}0$] and [$1\bar{2}10$] directions. The patterns correspond to AlN grown with (0001) planes parallel to the surface of the film. As the electron beam is rotated in the plane of the film, each pattern should exhibit a repeat period of 60° and the two patterns should alternate every 30°. Figure 2 shows the

FIG. 1

CALCULATED RED PATTERN FOR AlN OR ZnO

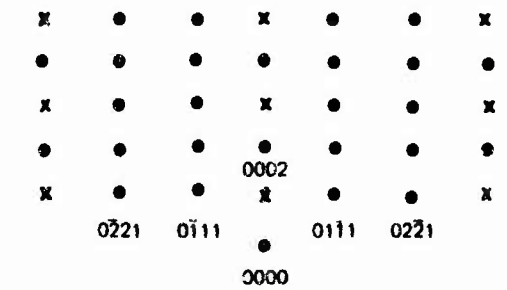

ELECTRON BEAM IN $[10\bar{1}0]$ DIRECTION

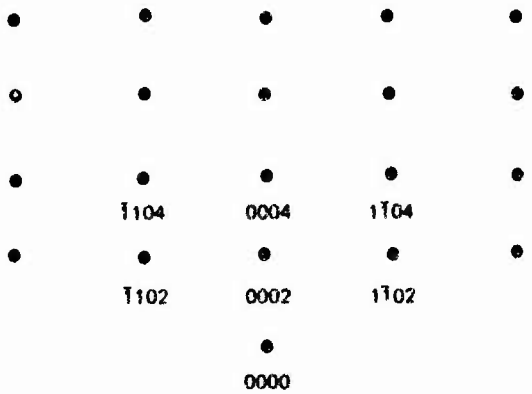

ELECTRON BEAM IN $[11\bar{2}0]$ DIRECTION

FIG. 2

RED OF AlN ON (0001) Al_2O_3

ELECTRON BEAM ALONG $[1\bar{1}00]$

ELECTRON BEAM ALONG $[11\bar{2}0]$

reflection electron diffraction patterns obtained for AlN grown on (0001) oriented aluminum oxide. Under rotation, the angular dependence of the diffraction patterns was found to vary as described above. In the diffraction experiments the electron beam is incident at a grazing angle and illuminates the full length of the film. Traversal of the sample over its full width in a direction orthogonal to the beam produced no variation in the diffraction pattern indicating that the film was indeed single. Diffractometer traces exhibited a single diffraction peak corresponding to a "d" spacing of 2.490Å. This value coincides with the spacing expected for (0002) planes of aluminum nitride.

Figure 3 depicts the expected diffraction patterns with the electron beam directed along the [0001] and [11$\bar{2}$0] zone axes for AlN with (11$\bar{2}$0) planes parallel to the surface of the film. Figure 4 shows the actual reflection electron diffraction pattern obtained for AlN grown on (1$\bar{1}$02) oriented aluminum oxide substrates. The [0001] and [11$\bar{2}$0] patterns alternate every 90° for a rotation of the beam in the plane of the film. The periodic behavior exhibits the proper symmetry. Diffractometer traces showed a single peak corresponding to a "d" spacing of 1.557Å which is that expected for (11$\bar{2}$0) planes of AlN. Yim, et al (Ref. 2) have reported that two other orientations were observed for single crystal AlN layers grown on (1$\bar{1}$02) sapphire, (30$\bar{3}$5) and (11$\bar{2}$7) AlN. These results were obtained by chemical vapor deposition. In our work only the (11$\bar{2}$0) orientation of AlN was obtained on (1$\bar{1}$02) sapphire substrates.

The single crystal films grown were generally clear and transparent but on occasion films with a hazy appearance were produced. Optical transmission measurements indicated that the optical cutoff in the ultraviolet occurred near 2000Å corresponding to a band gap of approximately 6.2 ev in agreement with the work of Yim, et al (Ref. 2).

The surface quality of the films grown by sputtering are generally superior to those obtained by chemical vapor deposition. It has been reported that surface acoustic wave devices fabricated with AlN films thicker than 1.6μ, which were grown by chemical vapor deposition, require mechanical polishing to remove the surface irregularities before definition of interdigital transducers can take place (Refs. 3, 4). Figures 5 and 6 are electron micrographs of replicated surfaces of 2.5 micron thick aluminum nitride films grown on (0001) and (1$\bar{1}$02) sapphire substrates. The surfaces obtained tend to mirror the surface imperfections of the polished substrates.

2.3 Surface Acoustic Wave Device Evaluation of AlN Films

A surface acoustic wave delay line was fabricated to evaluate the piezoelectric characteristics of the films grown by sputtering. To date the only published data on surface acoustic wave devices fabricated with AlN on sapphire is the work at North American-Autonetics. Their data is confined to AlN on (1$\bar{1}$02) sapphire substrates with the c-axis of the AlN lying in the plane of the film.

CALCULATED RED PATTERN FOR AlN OR ZnO

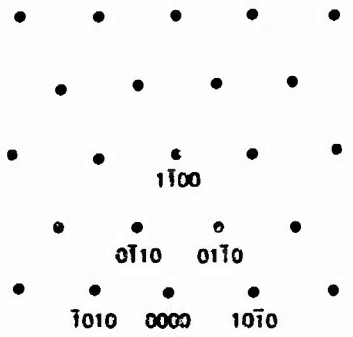

ELECTRON BEAM IN [0001] DIRECTION

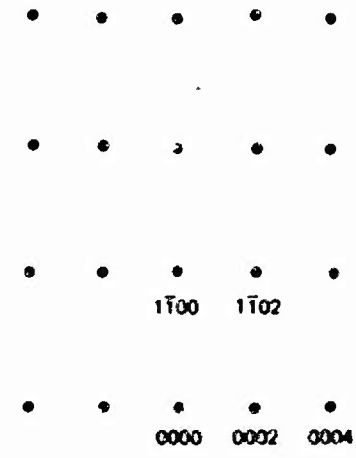

ELECTRON BEAM IN $[11\bar{2}0]$ DIRECTION

FIG. 4

RED OF AIN ON $(1\bar{1}02)$ Al_2O_3

(0001)

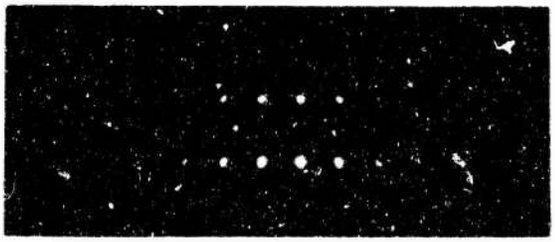

$(11\bar{2}0)$

FIG. 5

ELECTRON MICROGRAPH OF AIN ON (0001) Al_2O_3

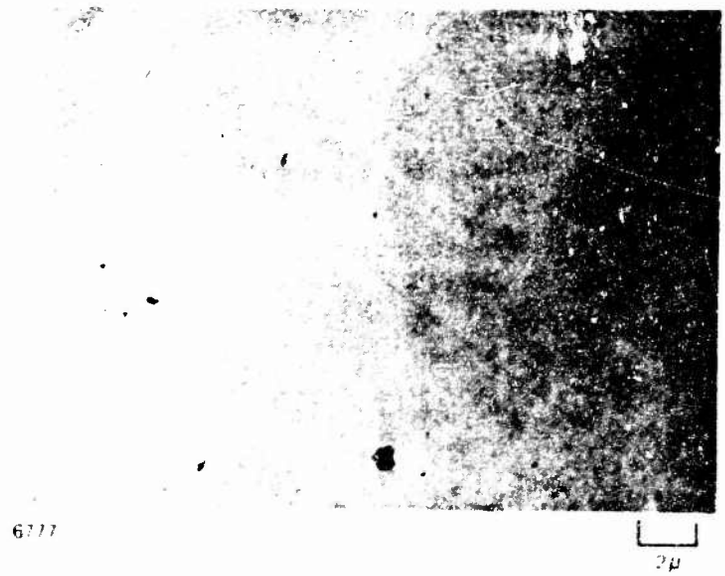

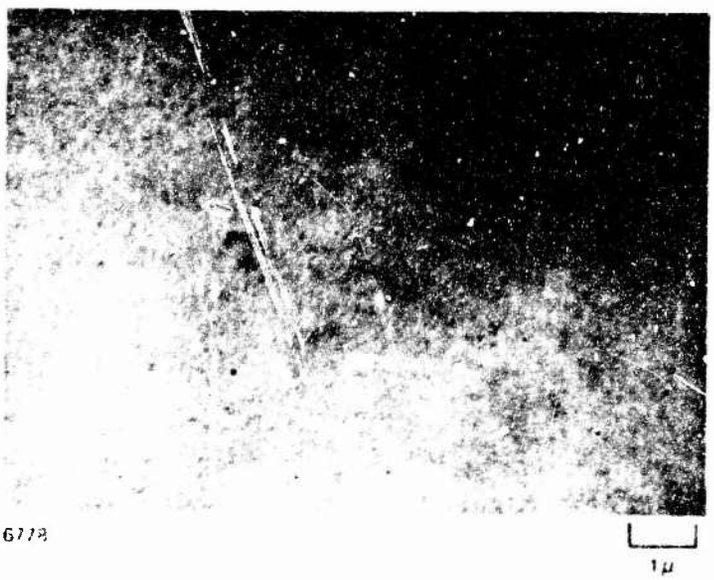

FIG. 6

ELECTRON MICROGRAPH OF AIN ON $(1\bar{1}02)$ Al_2O_3

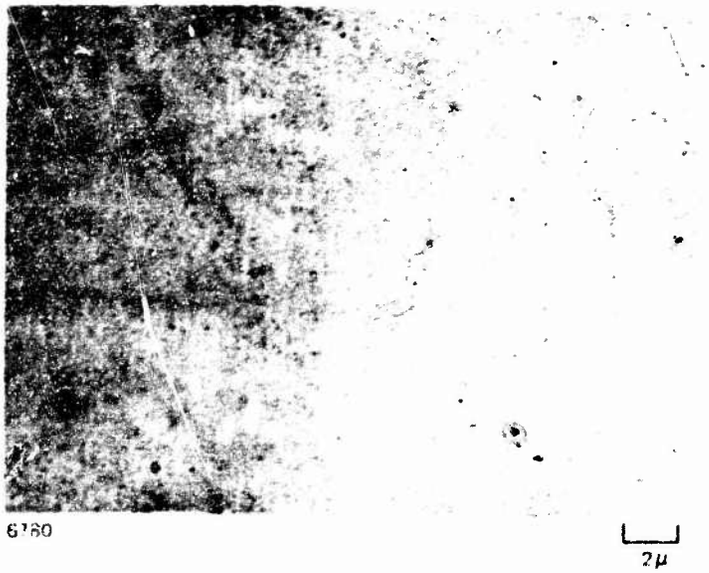

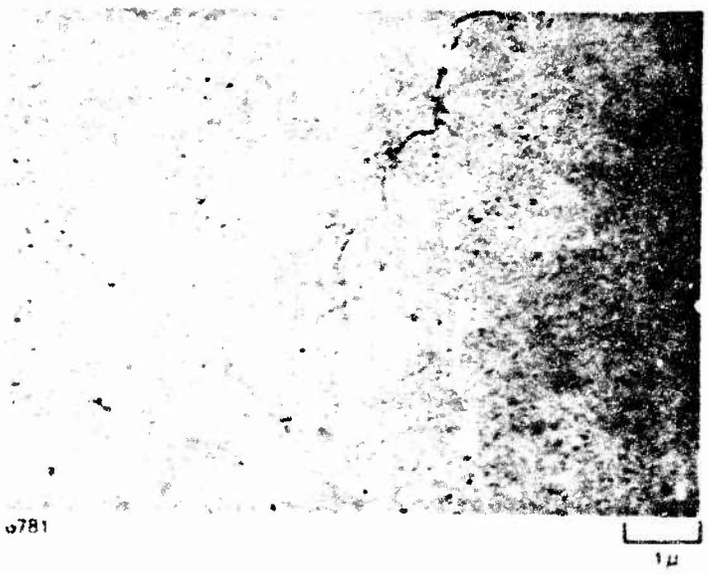

The data presented in our report is the first useful data for AlN grown on (0001) oriented sapphire (c-axis $\perp$ to the film plane). The advantage of this orientation for delay line construction is that the anisotropy (and delay line beam steering) is low in the (0001) plane, whereas with the c-axis in the plane of the film, the interdigital transducers must be aligned to propagate surface acoustic waves along the c-axis of the AlN.

The surface acoustic wave data presented below is for a 2 micron thick single crystal aluminum nitride film grown on a (0001) sapphire substrate. Interdigital (ID) transducers were photolithographically fabricated with the following specifications:

Pattern Spacing - 5.1 mm
Number ID Fingers - 21
Finger Length - 1 mm
ID Periodicity - 25 μm
Metallization - 0.15 μm aluminum

The surface acoustic wave transducer configuration is illustrated in Fig. 7, and Fig. 8 shows a plot of the input impedance versus frequency for the two transducers. The nearly identical response for the two transducers is indicative of the uniformity of film thickness. Transducer insertion loss as a function of frequency is shown in Fig. 9. The two port insertion loss was lowered from 68 dB to 37 dB at 216 MHz by series tuning with miniature inductors. In fact, the insertion loss would have been much lower, at least as low as 25 dB, if our transducer pattern had had low spurious shunt capacitance. This will be corrected in future experiments with a small bonding pad configuration. A pulse delay time for the above structure was measured to be 920 ns with a propagation loss of 1.5 dB for the path. The pulse echo response is shown in Fig. 10. The aluminum nitride dielectric loss Q was estimated to be 10, the dielectric constant approximately 10 and the resistivity greater than 10^5 Ω-cm. The surface acoustic wave velocity was determined to be 5500 m/s. The effective piezo coupling constant (k^2) was determined to be .08%. This compares very favorably with the value of .09% obtained at Autonetics (Ref. 3) for the same film thickness to transducer pattern periodicity utilized here.

The results obtained to date are very encouraging since the surface acoustic wave experiments were done with material prepared by a technique which is in its very early stages of development. The chemical vapor deposition process has several years of development.

2.4 Future Studies

The main emphasis to date has been directed toward achieving epitaxy of aluminum nitride. With this behind us, efforts will be aimed at refinements in the

FIG. 7

INTERDIGITAL TRANSDUCER

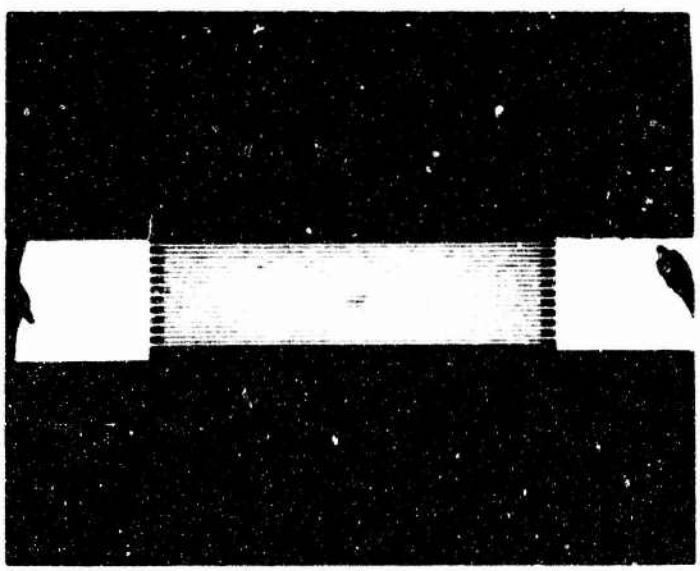

INPUT IMPEDANCE VS FREQUENCY FOR AIN-103
(SHOWS NEARLY IDENTICAL RESPONSE FOR THE TWO TRANSDUCERS)

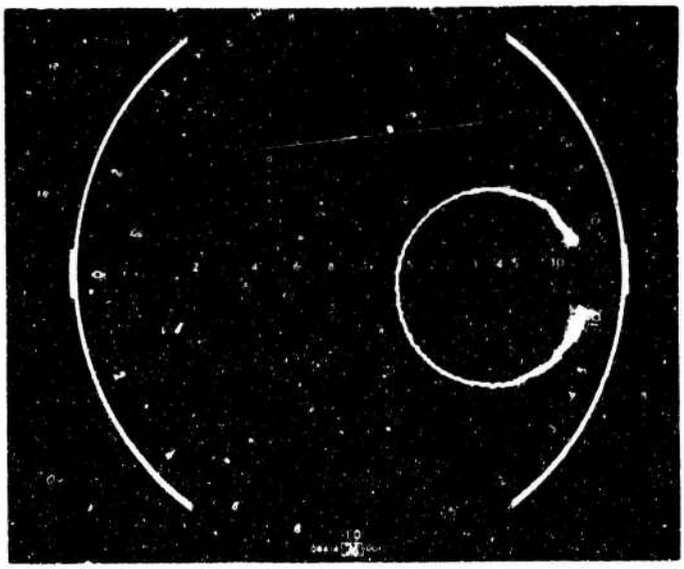

PORT 1

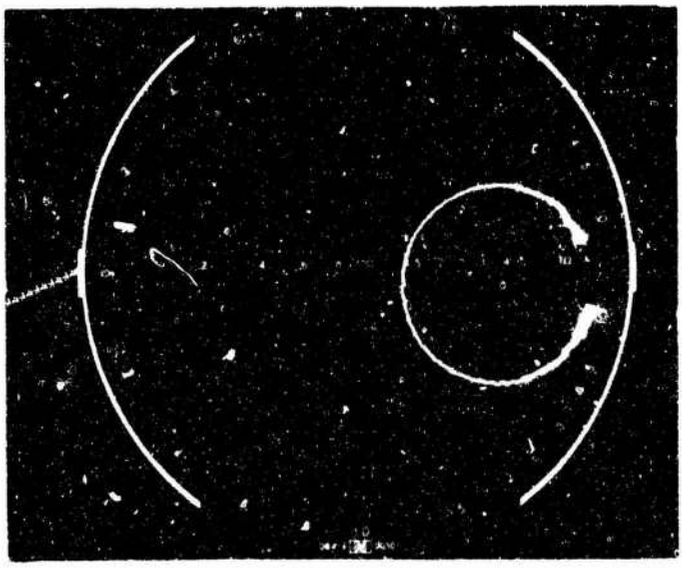

PORT 2

FIG. 9

TRANSDUCER INSERTION LOSS VS FREQUENCY FOR AlN ON (0001) SAPPHIRE

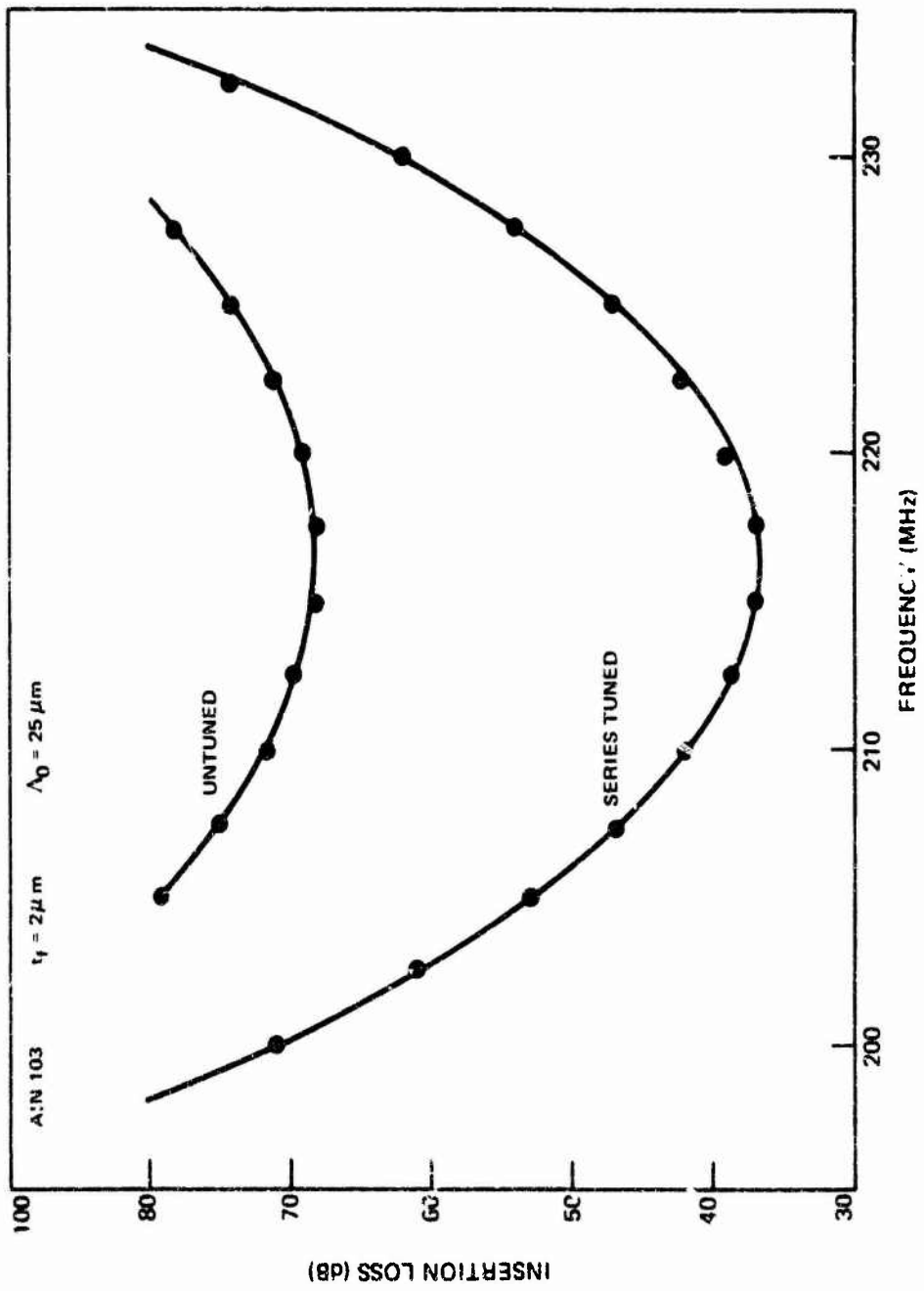

FIG. 10

PULSE ECHO RESPONSE OF AIN–103
(f = 216 MHz, IL = 37 dB, BW = 10 MHz)

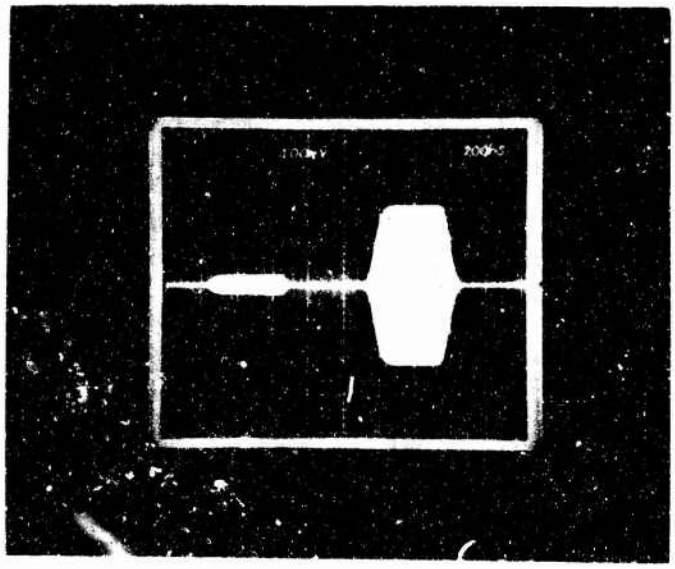

deposition parameters to optimize material properties in order that the eventual goal of fabricating thin film active integrated optic devices can be realized. Optical and electrical properties of the films will be more completely characterized. Attention will be focused on devices employing acoustooptic interactions. Preliminary experiments in the growth of gallium nitride will also be addressed.

3.0 SPUTTERED EPITAXIAL FILMS OF ZINC OXIDE

Zinc oxide is a II-VI semiconductor with the hexagonal wurtzite structure. It is isomorphous in structure to aluminum nitride. It is piezoelectric and electroluminescent and has considerable potential for integrated optics applications.

Single crystal films of zinc oxide have been prepared by the close-space vapor transport technique (Ref. 5) and also by dc sputtering (Ref. 6). The close-space vapor transport technique generally yields films of low resistivity and must be lithium diffused in order to raise the resistivity to acceptable values. A second drawback to this approach is that it yields films of poor crystallinity on (0001) sapphire substrates, and films of good crystallinity are only obtained on ($1\bar{1}02$) cut substrates.

Single crystal films have been grown by Rosgonyi and Polito (Ref. 6) by dc sputtering but only on (0001) oriented substrates of sapphire and CdS. The deposition rates for epitaxy were extremely low, approximately 200 Å/hr, too low to be practical. We report below not only the first epitaxial deposition of zinc oxide achieved on ($1\bar{1}02$) sapphire substrates by sputtering but also epitaxial growth of zinc oxide on (0001) oriented sapphire at practical rates (90 Å/min).

3.1 Epitaxial Thin Film Deposition of ZnO

Films of ZnO were prepared by rf sputtering from a 99.99% pure target of the compound in a 80% argon and 20% oxygen ambient. The argon was 99.999% pure and the oxygen was 99.994% pure. The sputtering chamber was pumped with a turbomolecular pumped backed with a standard mechanical pump. Pumping speed of the turbomolecular pump is about 250 liters per second in the millitorr range. Since the chamber has a volume of about 25 liters, this represents a change of sputtering gas about 10 times per second. The chamber is of stainless steel construction. Copper gasketed seals as well as viton A "O" ring seals are used. The system typically was evacuated to about 2×10^{-6} torr before deposition began.

Substrates were heated by placing them on a thin high purity Al_2O_3 slide which was in direct contact with a tantalum strip heater. The heater temperature was monitored with a chromel-alumel thermocouple spot welded to the heater. The correlation between the heater temperature and substrate temperature is presented in Appendix I.

The sputtering gas was admitted through two precision micrometer valves. The argon flow was first adjusted to yield a pressure 80% of the total desired sputtering pressure, and then the oxygen flow was adjusted to bring the pressure up to 100% of the desired pressure.

The substrates were of the same type and prepared in the identical manner as described in Section 2.1 of this report.

Epitaxy was achieved on (0001) oriented sapphire for the following conditions:

Total gas pressure	- 10 mtorr
Substrate temperature	- 600°C
Deposition rate	- 90 Å/min
Target input power density	- 0.7 watts/cm^2

Epitaxy was achieved on the $(1\bar{1}02)$ oriented sapphire for the following conditions:

Total gas pressure	- 100 mtorr
Substrate temperature	- 700°C
Deposition rate	- 33 Å/min
Target input power density	- 2.2 watts/cm^2

A special feature of this sputtering system is the variety of magnetic fields which can be produced in the region of the substrate and cathode. The fields are produced by a pair of solenoids each about $\frac{1}{2}$ inch long, $1\frac{1}{2}$ inches thick and 7 inches in diameter. The coils are concentric to the cathode and substrate holder. Spacing between the coils and position of the coil pair midplane are variable over a range of about 6 inches. The target-to-substrate distance is also variable but was maintained at 1-1/8 inches for these experiments. The coils can be connected so that their fields either add or oppose. In this way the fields can be changed from a predominantly axial one to a quadrupole one. A number of experiments have been made to determine the effect of these fields on the substrate temperature and film deposition uniformity. The configuration chosen for these experiments was with the electromagnet coils arranged to produce a predominantly axial field. This configuration produced a reasonably uniform deposition over the central 2 inches of the substrate holder and at the same time minimized the substrate heating over the same range by diverting the energetic secondary electrons emitted from the target. At a target power density of 2.2 watts/cm^2, it is estimated that the increase in substrate temperature above that implied by measuring the substrate heater was 100°C. While at the target power density of 0.7 watts/cm, the increase in temperature was only 25°C. Without the pressure of the magnetic field the increase in temperature would have been 180°C and 75°C, respectively. Another equally important aspect of diverting the secondary electrons from interacting with the substrate is their effect on the texture of the film. Films grown outside of the central 2 inches have a cloudy grainy appearance. The same effect is noted at zero or low magnetic fields for films grown at the center of the substrate holder. The films grown in the center of the substrate with high axial fields, however, are smooth and clear.

3.2 Characterization of ZnO Films

The film structure was determined using x-ray diffraction and reflection electron diffraction. Zinc oxide is isomorphous to the structure of aluminum nitride and their respective lattice parameters are within a percent of each other. Therefore, Figs. 1 and 3 also represent the expected electron diffraction patterns for single crystal zinc oxide films. Figures 11 and 12 show reflection electron diffraction patterns obtained for films grown on (0001) and ($1\bar{1}02$) sapphire substrates. The epitaxial relationships between film and substrate are found to be:

$$(0001)ZnO \parallel (0001)Al_2O_3,\ [1\bar{1}02]ZnO \parallel [11\bar{2}0]Al_2O_3$$

$$(1\bar{1}02)ZnO \parallel (1\bar{1}02)Al_2O_3,\ [0001]ZnO \parallel [1\bar{1}0\bar{1}]Al_2O_3$$

The surface quality of the films is excellent and tends to replicate the substrate finish whereas chemical transport produces generally rough films. Figure 13 is an electron micrograph of a replicated surface of a one micron thick zinc oxide film deposited on ($1\bar{1}02$) sapphire. The films grown are clear and transparent.

The resistivity of the sputtered films is 10^6 Ω-cm or better. No lithium diffusion is required to enhance the resistivity in contrast to films prepared by chemical vapor deposition techniques.

3.3 Surface Acoustic Wave Device Evaluation

The performance of the zinc oxide films grown on ($1\bar{1}02$) sapphire substrates was evaluated using the same interdigital transducer structure described in Section 2.3. The film thickness was 1.4 μm; therefore, the surface acoustic wave velocity was strongly affected by the sapphire substrate. Transducers were placed to propagate acoustic waves parallel and perpendicular to the c-axis of the zinc oxide (see Fig. 14). The minimum untuned two port insertion loss was 43 dB for propagation along the c-axis. Perpendicular to the c-axis the insertion loss was 22 dB higher.

The acoustic resonant frequency was determined to be 215 MHz.

The transducer insertion loss as a function of frequency is shown in Fig. 15 for the interdigital transducer pattern aligned to propagate surface acoustic waves along c-axis of the zinc oxide. The piezoelectric coupling coefficient k^2 was measured to be approximately 0.4%.

This is subsequently higher than the value of 0.31% (Ref. 4) reported for zinc oxide films on sapphire prepared by the close-space transport method. The measured

FIG. 11

RED OF ZnO ON (0001) Al_2O_3

$[10\bar{1}0]$

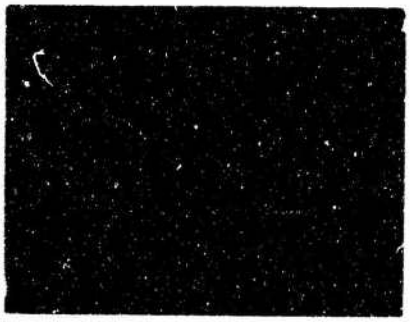

$[11\bar{2}0]$

FIG. 12

RED OF ZnO ON $(1\bar{1}02)$ Al_2O_3

(0001)

(1120)

FIG 13

ELECTRON MICROGRAPH OF ZnO ON $(1\bar{1}02)$ Al_2O_3

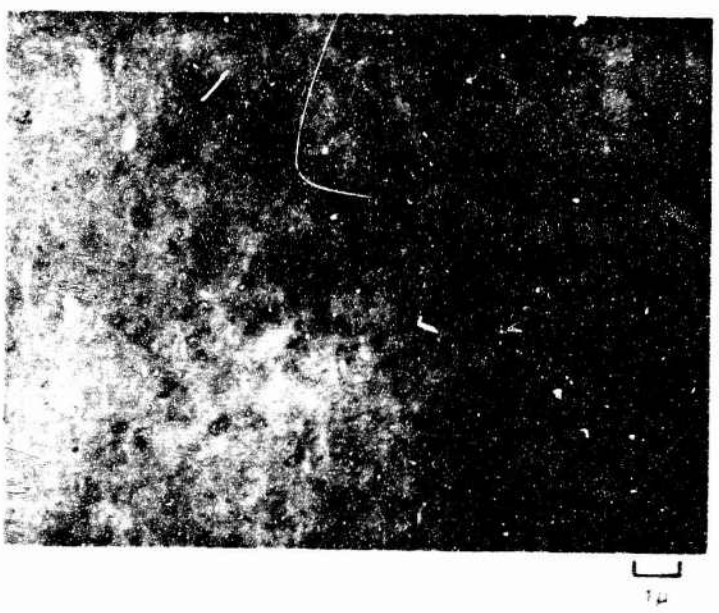

FIG 14

SURFACE ACOUSTIC WAVE TRANSDUCER PATTERNS ON $(11\bar{2}0)$ ZnO

FIG. 15

UNTUNED INSERTION LOSS VS FREQUENCY
FOR SINGLE CRYSTAL ZnO FILM ON SAPPHIRE ($11\bar{2}2$)

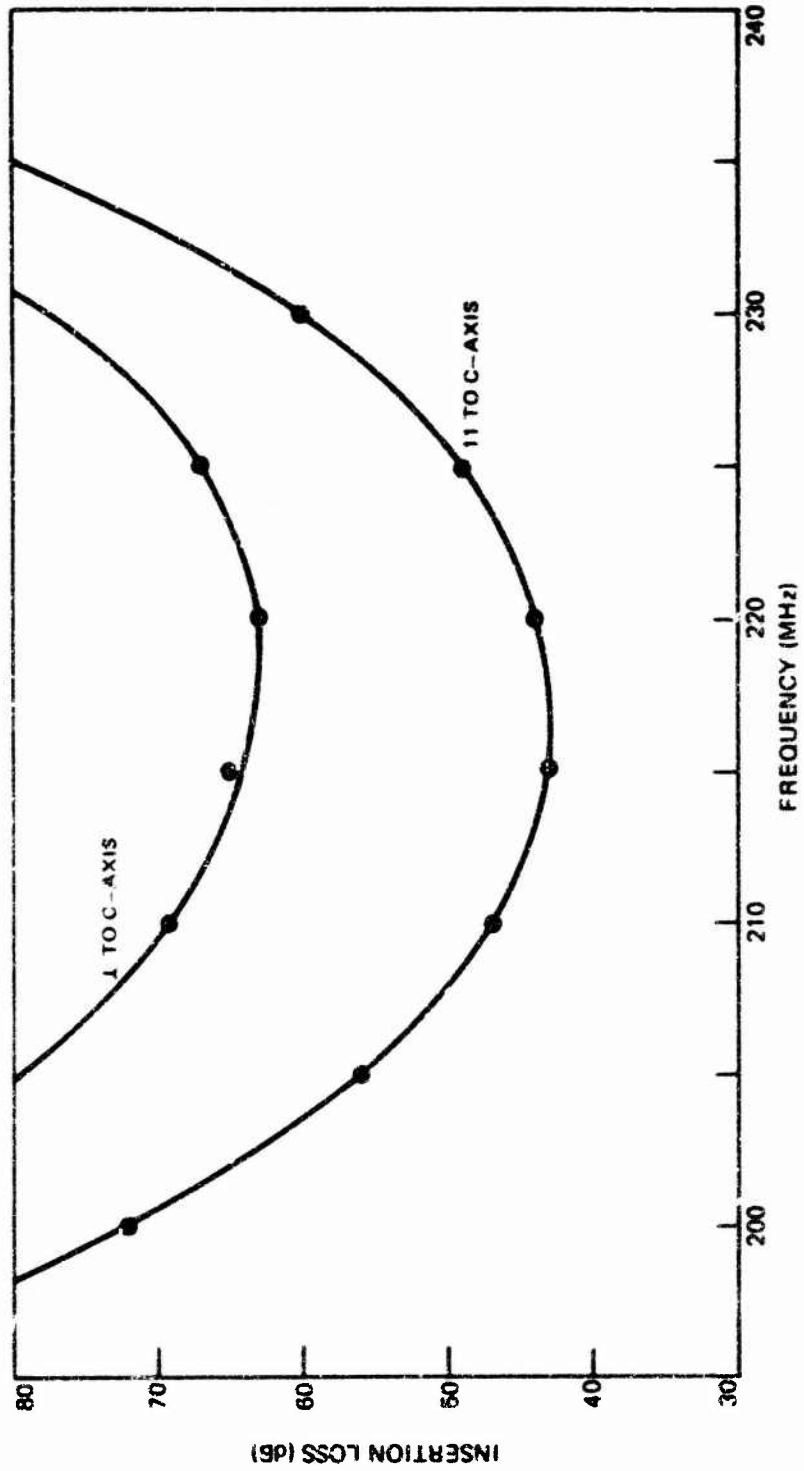

surface acoustic wave velocity was 5100 m/sec. This compares favorably with the calculated value of Lim (Ref. 7) for zinc oxide on sapphire for the film thickness to transducer pattern periodicity ratio (.056).

3.4 Future Studies

As with the other materials studied in this program, the main emphasis on ZnO has been to determine a set of epitaxial sputtering parameters. Future work will include investigation and optimization of these films for properties of interest for use in integrated optics applications.

4.0 GROWTH OF EPITAXIAL GALLIUM ARSENIDE FILMS

Single crystal epitaxial films of gallium arsenide have been reactively sputtered onto gallium arsenide substrates. These films should be useful in a variety of applications such as integrated optics, acousto-electric, and microwave devices. The films were reactively sputtered from a gallium target by arsenic ions. A practical pressure of arsenic was maintained by heating the vacuum chamber to ~ 250°C to prevent arsenic condensation and heating high purity arsenic in an alumina crucible. The use of arsenic as the sputtering gas should improve the stoichiometry of the sputtered gallium arsenide film. This is due to the high vapor pressure of arsenic at the temperatures required for epitaxy.

The electrical and optical properties of the films are being determined, and the results to date are included in this report.

4.1 Verification of Gallium Arsenide Synthesis by Reactive Sputtering

4.1.1 X-Ray Diffraction

A Phillips X-ray Diffractometer with a copper target was used in this investigation. The target was excited by 40 Kev electrons, and a nickel filter was inserted into the x-ray beam. An x-ray diffraction scan of a single-crystal gallium arsenide substrate is shown in Fig. 16a. The substrate is oriented with a (100) face parallel with the surface, and therefore, large peaks due to the (200) and (400) planes are recorded. Figure 16b is a diffractometer scan of a sputtered film on another (100) oriented gallium arsenide substrate. The large (200) and (400) peaks are principally due to the substrate, but all the other peaks result from the polycrystalline film indexed to be gallium arsenide. No other materials or phases were observed.

4.1.2 Electron Microprobe Analysis

Using a Norelco electron probe, two polycrystalline samples were quantitatively analyzed and were found to be stoichiometric to within 0.5 to 1% which is the accuracy of the method.

The samples were also microprobe analyzed for impurities. Specific analysis was made for those materials used in the vacuum system, that is, Fe, Ni, Cr, Cu, Si and O. These elements were not observed down to the sensitivity of the measurement which is about 0.1 weight percent. A full spectral check was made for all the other detectable elements, but this measurement did not reveal any other impurities.

FIG. 16

X – RAY DIFFRACTION SCANS

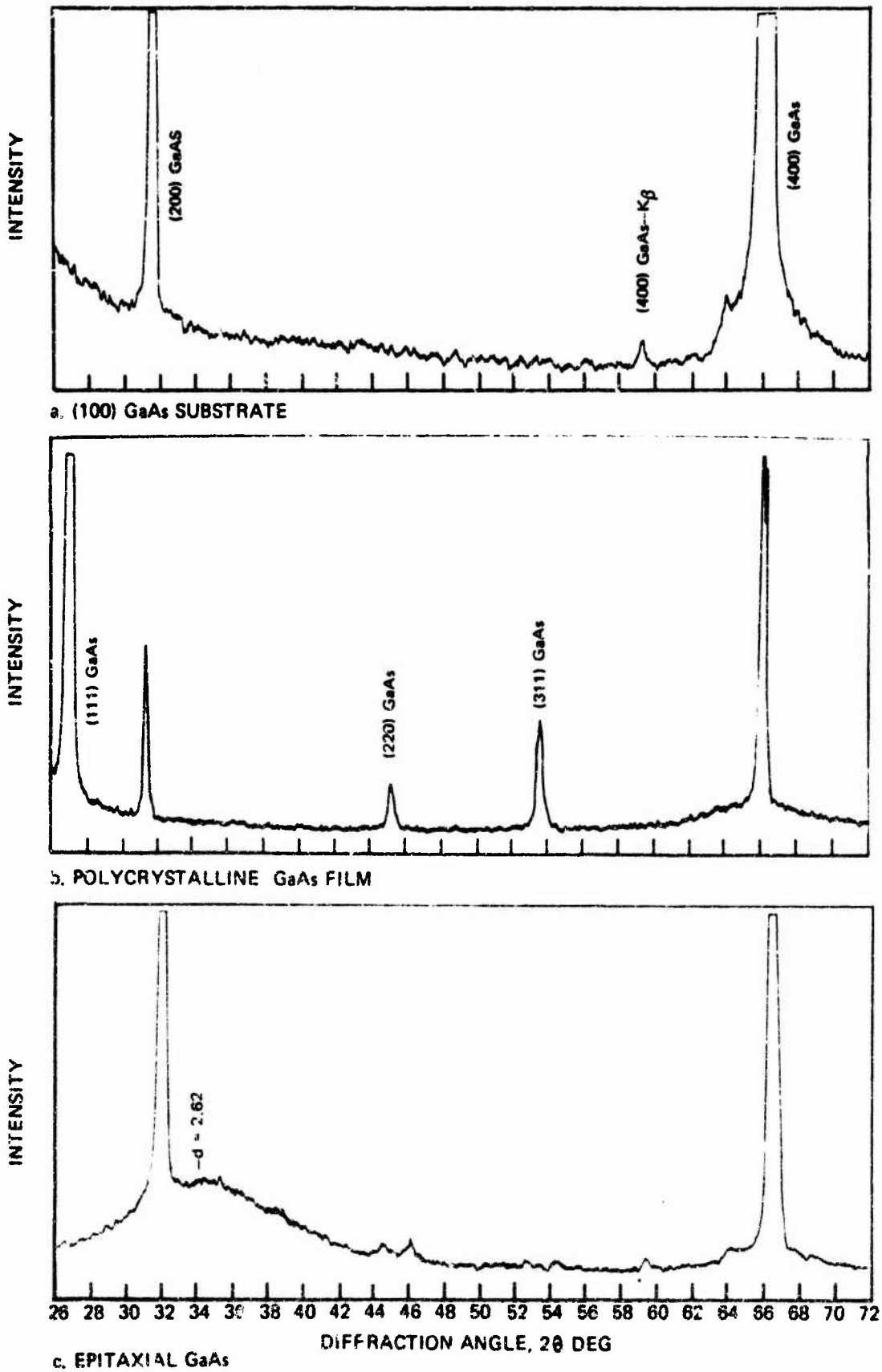

4.1.3 Infrared Spectrographic Analysis

A Perkin-Elmer Type 621 infrared spectrophotometer fitted for reflectance measurements was employed in this phase of the investigation.

The reststrahlen peak was used to identify the presence of GaAs deposited on a silicon substrate. The silicon substrate was chosen since there is no change in its reflectivity in the 30- to 40-μm range. An almost identical reflectance peak was found for the GaAs film as is seen for bulk chromium-doped semi-insulating GaAs (compare Figs. 17a and 17b).

Subsequent films grown on GaAs substrates gave rise to very large interference fringes, a typical example of which is seen in Fig. 17c. This could only happen if there was a large difference in the index of refraction between the film and substrate, or if an interfacial layer, with a different index, existed between the GaAs substrate and the film. Examination of Fig. 17c also reveals a periodic amplitude variation with wavelength which suggests the presence of a second film.

4.2 Verification of the Presence of an Interfacial Layer

Two techniques were employed to determine if such a layer existed. First, a substrate was mounted in cross section, lightly etched and replicated. The replica was then observed in an electron microscope. The photomicrograph in Fig. 18 clearly shows an interface layer between the substrate and the GaAs deposit. Second, another sample was etched slowly down from the surface until the interface layer was revealed. A photograph of this layer is shown in Fig. 19, where the interface layer has folded over. Another sample of the interface layer was floated off this GaAs substrate and placed on a silicon wafer. Electron microprobe analysis of this film indicated only gallium and oxygen; therefore, the interfacial layer is most probably Ga_2O_3.

Contamination of the gallium target by oxygen and water vapor occurs when the vacuum system is opened. The films discussed above were deposited directly from this contaminated target; consequently, the interface layer of gallium oxide is formed as the oxidized target surface is sputtered. When all the oxide is sputtered from the target, a distinct gallium arsenide layer is deposited on the oxide layer as can be seen in Fig. 18 and as verified by x-ray diffraction.

4.3 Techniques to Eliminate the Interface Layer

The preceeding experiments have determined the existence of an oxide layer on the substrate. This layer was the cause of polycrystalline growth and must be eliminated to enable epitaxial growth.

IR REFLECTANCE SPECTROGRAPHS

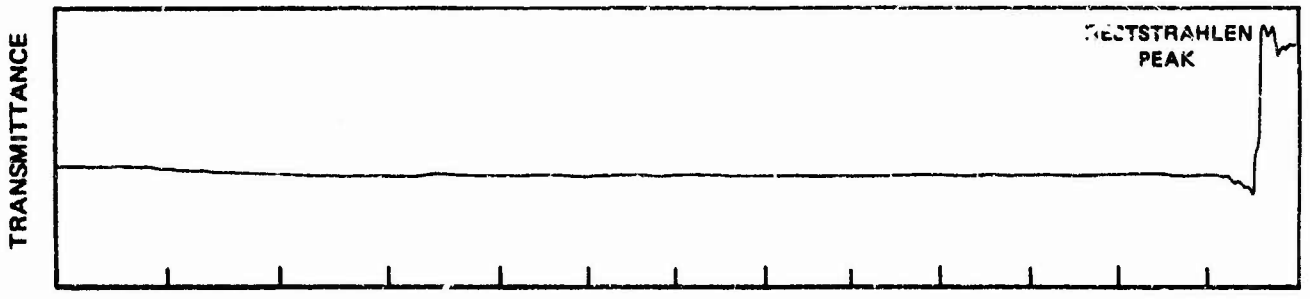

a. BULK CHROMIUM-DOPED GaAs

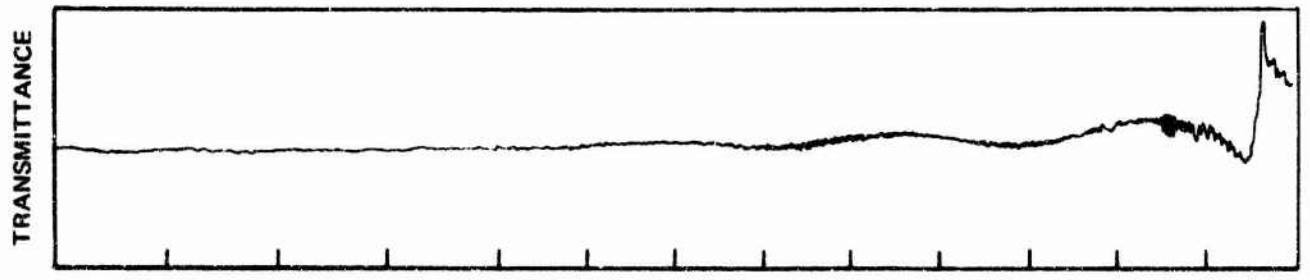

b. GaAs FILM ON SILICON

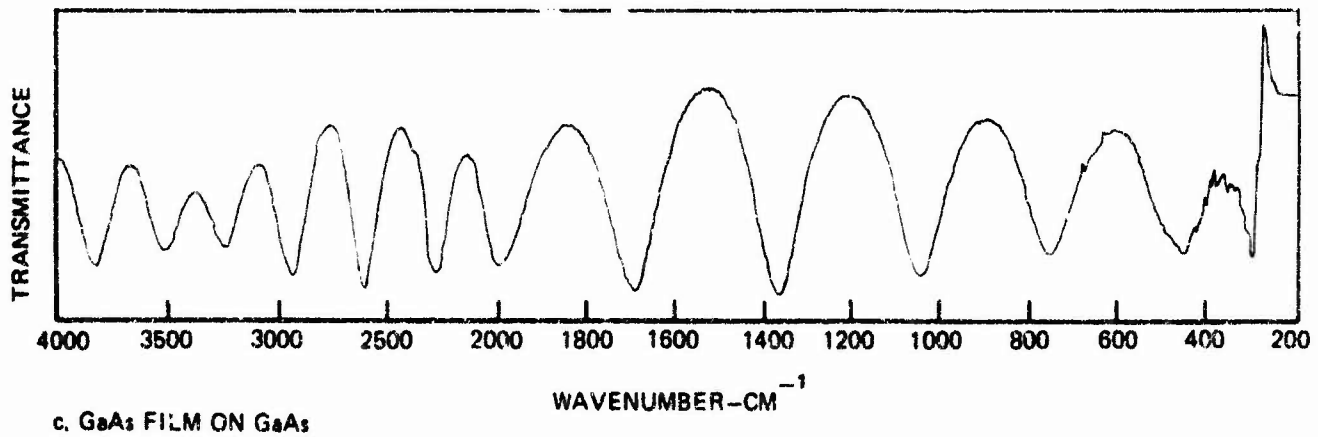

c. GaAs FILM ON GaAs

FIG. 18

ELECTRON PHOTOMICROGRAPH OF GALLIUM ARSENIDE AND SPUTTERED LAYERS

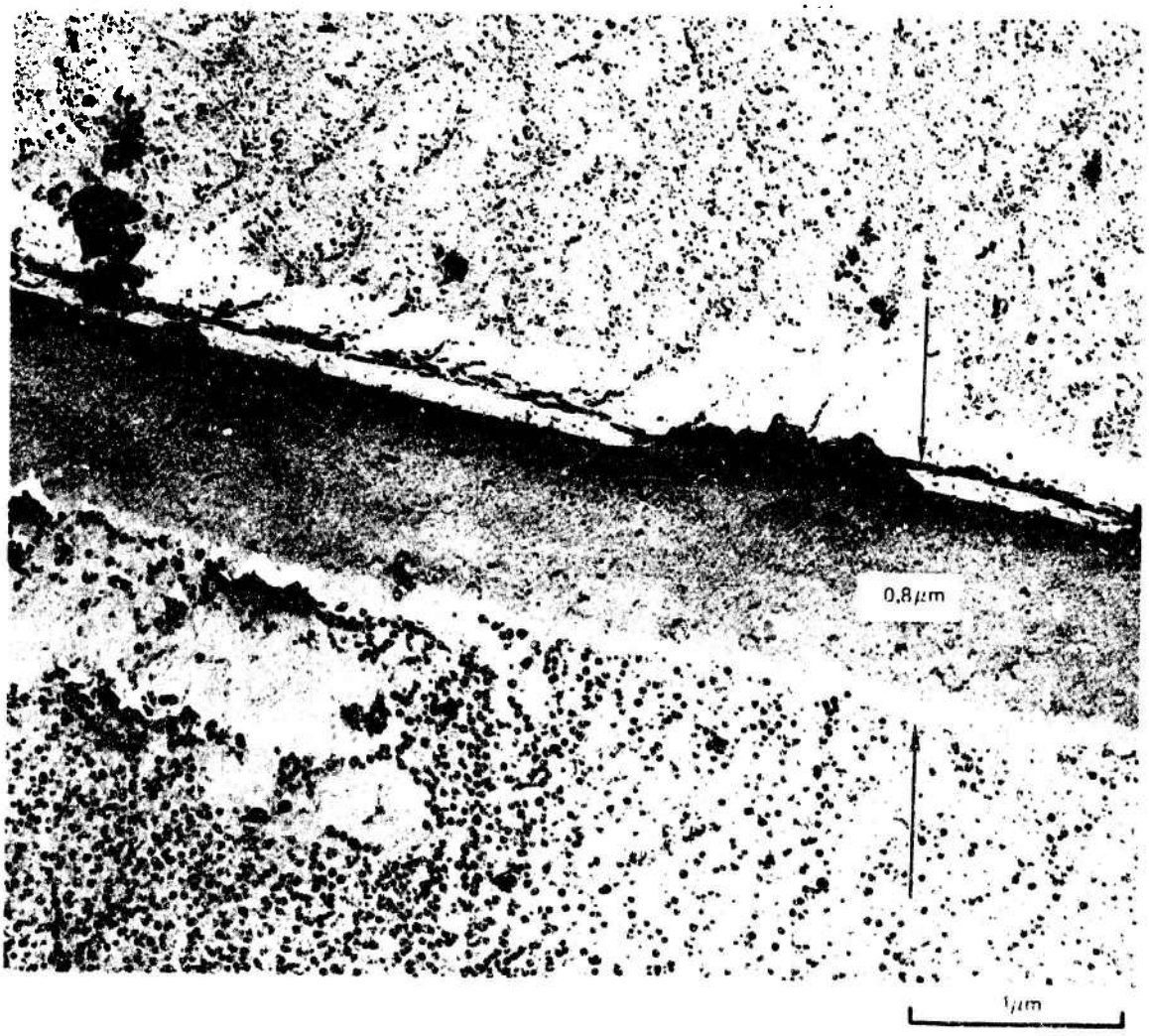

FIG. 19

OPTICAL PHOTOMICROGRAPH OF THE TOP VIEW OF THE INTERFACE LAYER

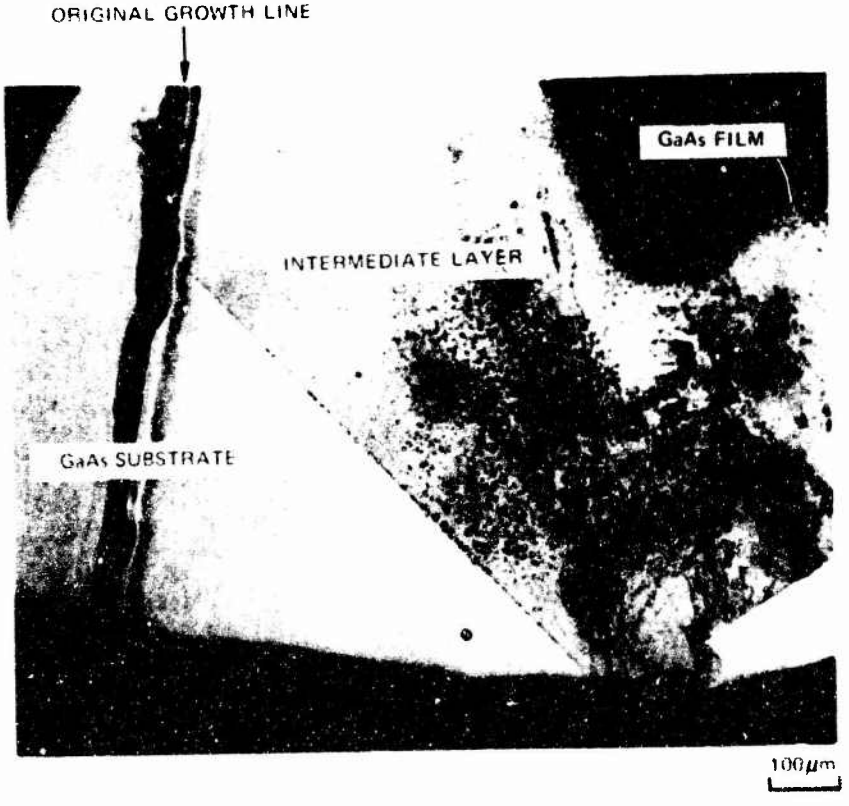

Two procedures have been employed which together have solved the problem of the interface layer. First, the gallium target is sputter cleaned with a shutter positioned in front of the substrate. This removes the gallium oxide from the target surface. Second, the shutter is opened and the substrate is sputter cleaned to remove any contamination that might have occurred during system bake-out and target cleaning. The use of these procedures enabled the deposition of an epitaxial film which is described in the next section.

Considerable engineering was required to introduce both a movable shutter and the capability of sputter cleaning the substrate. This was due to the presence of the two outer shrouds and the high temperature ($\sim 250^{\circ}C$) of the chamber.

4.4 Initial Epitaxial Results

4.4.1 Deposition Parameters

After the modification mentioned in the previous section were made, an epitaxial gallium arsenide film was deposited. The following process parameters were used:

1. Gallium target sputter cleaning - 15 W/cm^2 for 15 min.
2. Substrate rf sputter cleaning - 220 V (rms) for 12 min.
3. Film deposition - 3.7 W/cm^2 for 82 min.
4. Substrate temperature - $\sim 350^{\circ}C$.
5. Deposition rate - 244 Å/min.
6. Arsenic pressure - 25 mtorr.
7. Substrate - Cr-doped GaAs oriented in the (100) direction.

4.4.2 Reflection Electron Diffraction (RED)

Each of the samples were mounted on a pedestal using silver paint. The edges of the substrate were also covered with paint to prevent diffraction off the substrate. The (110) pattern from the film can be seen in Fig. 20. The computed "d" spacing is proper for gallium arsenide, and the orientation of the patterns with respect to the substrate cleavage planes is correct. Kikuchi lines, which indicate a high degree of order, are present for all orientations of the film with the electron beam. No evidence of polycrystalline rings, amorphous halos or twinning can be observed.

These RED results strongly indicate that the film surface is single crystal gallium arsenide which is epitaxially grown on the substrate.

4.4.3 X-ray Diffraction

The x-ray scan shown in Fig. 16c for the epitaxial sample has very large (200) and (400) peaks due to both the substrate and the film. There are also very weak

RED OF EPITAXIAL GaAs GROWN ON (100) GaAs SUBSTRATE

ELECTRON BEAM ALONG [110]

GaAs lines associated with (311) and (220) planes parallel to the sample surface. This indicates polycrystalline growth somewhere in the film. Together with the RED results it is presently believed that the polycrystallinity arises due to initial growth on dirt particles. The x-ray diffraction scan also has a broad amorphous peak around a "d" spacing of 2.62Å. This may also be associated with particles on the surface prior to deposition.

4.4.4 Conductivity and Hall Measurements

The conductivity was determined for a single crystal film grown on a chromium-doped GaAs semi-insulating substrate over the temperature range -100°C to 130°C. Due to the high impedance of the sample ($\sim 10^8$ ohms) dc measurements were made using a Keithley electrometer. Sample preparation involved defining a Hall mesa by etching through the film. Tin contacts were alloyed to the epitaxial layer, but this process also makes contact to the substrate. The resistivity of chromium-doped gallium arsenide is $\sim 10^8$ ohm-cm at room temperature and decreases rapidly with increasing temperature, $\rho \sim \exp(\Delta E/kT)$ where $\Delta E \sim 0.57$ eV (Ref. 8) in our temperature interval of measurement. Resistivity measurements made on our epitaxial layer and substrate above room temperature (see Fig. 21) show an activation energy (0.63 eV) characteristic of the substrate and not the film. At lower temperatures the substrate becomes more insulating and properly isolates the film to give meaningful film resistivity data. At room temperature the film resistivity is 9.3×10^3 ohm-cm and exhibits a resistivity variation with temperature of $\exp(0.085\ \text{ev}/kT)$. If the reasonable assumption is made that the carrier mobility does not change appreciably over this temperature interval, this temperature dependence can be due to a structural defect (Ref. 9) or to an impurity, e.g., copper (Ref. 10) or manganese (Ref. 11). If levels deeper than 0.1 ev below the conduction band are present, these of course, would be masked by the shorting-out effect of the substrate at higher temperatures.

At this point no reliable Hall data is available for the epitaxial material. If one calculates the Hall mobility and carrier concentration from our results at room temperature and assigns these values to the epitaxial layer, the results are as follows: free electron density, $n = 7 \times 10^{13}$ cm^{-3} and Hall mobility, $\mu_H = 9.7$ cm^2/V-sec. Since typical Hall measurements for the Cr-doped substrate material indicate a net n-type conductivity with Hall mobilities $\sim$ 100-600 cm^2/V-sec, significant contributions from the substrate to the measured Hall voltages will exist if the Hall mobility of a fairly resistive film is below that of the semi-insulating substrate. This is believed to be the situation here. Furthermore, a Hall mobility of 9.7 cm^2/V-sec for electrons does not make sense in GaAs. However, it is possible that the epitaxial film is p-type and has a Hall mobility less than commonly observed room temperature values of $\sim$ 400 cm^2/V-sec for pure material. The measured Hall voltage will then consists of a negative contribution from the substrate and a positive contribution from the film and not give a meaningful result if assigned to the film. The hole concentration at room temperature, assuming a reasonable hole mobility of 100 cm^2/V-sec and using the film resistivity of 9.3×10^3, is calculated to be

FIG. 21

RESISTANCE VS. INVERSE TEMPERATURE FOR EPITAXIAL GaAs ON SEMI-INSULATING SUBSTRATE

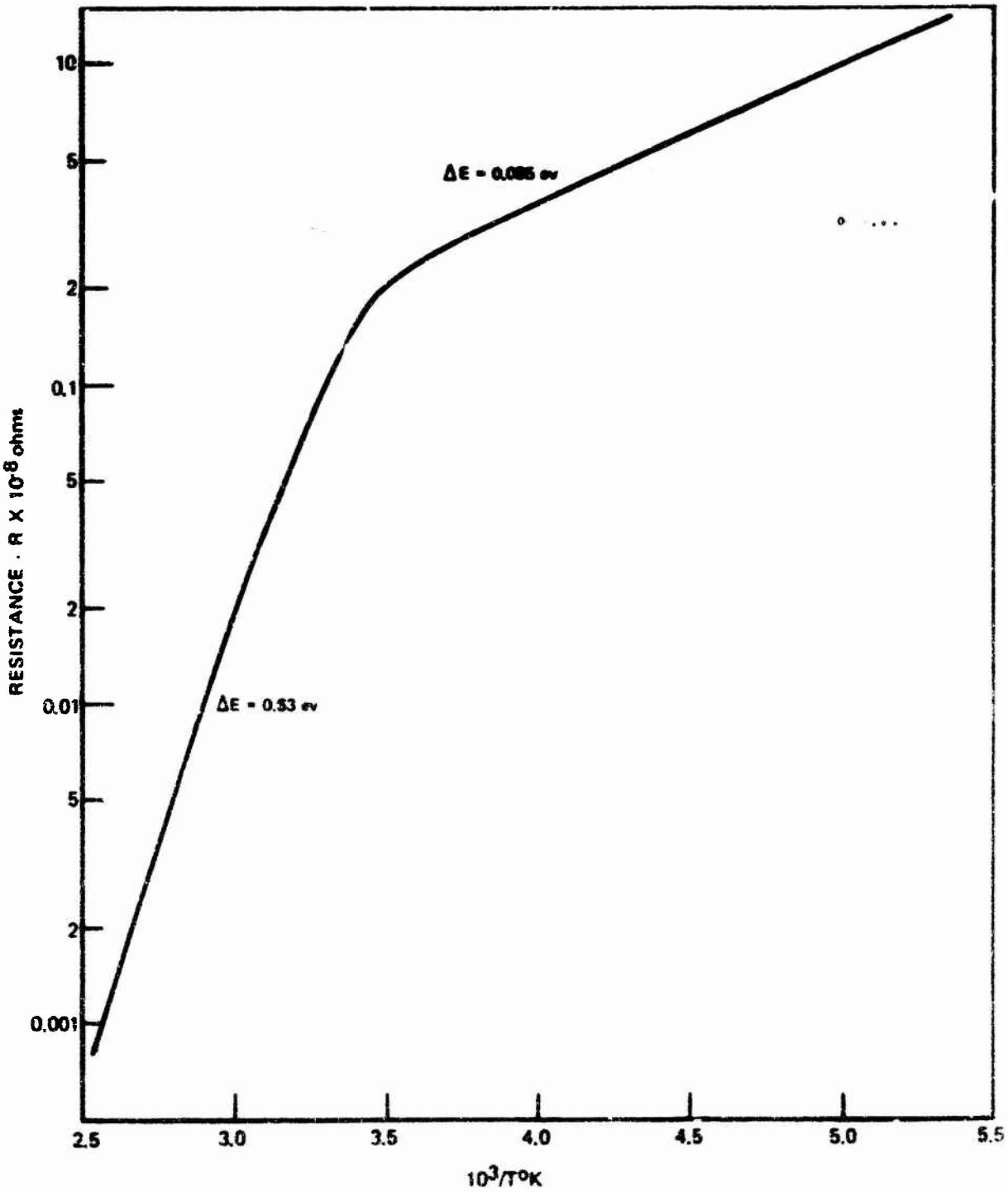

$\sim 6.7 \times 10^{12}$ cm^{-3}. Experiments are in progress to grow the GaAs epitaxial layer on insulating substrates, i.e., sapphire, and so isolate the GaAs mesa for Hall measurement. Alternatively, a thick layer, about 2 mils thick can be grown on semi-insulating GaAs, and the substrate removed by lapping. Unfortunately, using growth rates observed for GaAs up to now, this would require 30 hours of time and multiple growth runs. If single crystal growth cannot be obtained on non-GaAs insulating substrates, this will be our only recourse in order to fully electrically characterize the epitaxial material.

4.5 Conclusions and Future Work

There are two probable reasons for the observed properties of the first epitaxial GaAs film. The most ambiguous results are the high resistivity ($\sim 10^4$ ohm-cm) and the apparent low n-type mobility (~ 10 cm^2/V-sec). These imply a free carrier density of 7×10^{13} cm^{-3}. On the other hand, a mobility of 10 cm^2/V-sec implies ionized impurities greater than 10^{20} cm^{-3}. This indicates an extremely high level of compensation. The question then is whether these compensating species are principally impurities or arsenic and/or gallium vacancies. Electron microprobe analysis indicates impurity levels less than 10^{19} cm^{-3}. One might therefore conclude that the compensation is due to vacancies rather than impurities. Since the present mobility measurements are in doubt due to the canceling effect of the substrate in the net measured Hall voltage, it is impossible to draw any hard conclusions at this time. Attempts to grow gallium arsenide on sapphire are being made so that unambiguous mobility measurements can be made. If these results indicate a low mobility, then vacancies probably are the controlling factor. It will then be necessary to vary deposition rate, substrate temperature and arsenic pressure in an attempt to reduce the vacancy concentration. Whether the electrical properties are governed by p-type impurities or vacancies, n-type material can be produced by doping the layer by introducing an impurity such as tin into the gallium target. At some level of doping the films will convert to n-type with higher mobility. This can then be used as a measure of the intrinsic impurity or vacancy concentration if single crystal gallium arsenide cannot be deposited on the sapphire substrate. If the electrical properties are determined by several impurities present at 10^{18} cm^{-3} levels, this technique will determine their combined concentration. If the Hall results on sapphire indicate a mobility which corresponds to impurity levels of 10^{17} or 10^{18} cm^{-3}, then either impurities or vacancies may again be the controlling factor. A more sensitive chemical analysis such as ion microprobe mass spectrometry or neutron activation analysis will be needed to resolve the anomoly.

After the fundamental electrical and structural properties of the gallium arsenide layers have been established an attempt will be made to fabricate a device consistent with these properties.

Once the gallium arsenide has been characterized an aluminum target will be installed in the sputtering system and attempts will be made to deposit aluminum arsenide films on GaAs substrates.

5.0 REACTIVELY SPUTTERED EPITAXIAL RUTILE FILMS

The rutile modification of titanium dioxide is known to have one of the highest dielectric constants (90 $\perp$ and 180 $\parallel$ c-axis) (Ref. 12) among the simple oxides. The preparation of the rutile form of titanium dioxide is complicated by the fact that there exist two other polymorphic forms of the oxide, anatase and brookite. In many cases, the variation in the measured properties reported on thin film titanium dioxide is due in large measure to the fact that the films deposited are generally comprised of mixed phases of titanium dioxide. Goshtogore and Morieka (Ref. 13) have been able to successfully prepare epitaxial films of rutile by chemical vapor deposition utilizing the reaction of titanium tetrachloride and oxygen. We believe that the present work is the first successful effort in obtaining epitaxial single crystal films of rutile by reactive rf sputtering.

5.1 Epitaxial Thin Film Deposition of TiO_2

Films of rutile were prepared by reactive rf sputtering of a titanium target in oxygen. The titanium target was 99.999% pure and the oxygen was 99.994% pure. The sputtering chamber was of stainless steel, pumped with a conventional oil diffusion pumped and backed with a standard mechanical pump. A liquid nitrogen cooled chevron baffle and a water cooled chevron baffle were located between the chamber and the diffusion pump. All vacuum ports were sealed with viton A "O" rings. The system was evacuated to approximately 2×10^{-6} torr before each run.

The initial efforts to achieve epitaxy were directed toward growing rutile on rutile. Rutile substrates were cut with the c-axis normal to the surface. Epitaxy was obtained at a substrate heater temperature of 650°C, an oxygen pressure of 10^{-2} torr and power density of 1.6 W/cm^2. Under similar conditions, epitaxy was not achieved on $(1\bar{1}02)$ and (0001) oriented sapphire substrates. The stainless steel substrate heater was strongly oxidized at higher temperatures and was replaced with a tantalum heater.

Substrates were heated by placing them either directly onto a tantalum strip heater or on a thin high purity Al_2O_3 slide which was in direct contact with the heater. The temperature of the heater was monitored with an optical pyrometer at temperatures above 800°C and with a chromel-alumel thermocouple spot welded to the heater at temperatures below 800°C. Agreement between the two was within 5°C at 800°C. Above 800°C the thermocouple weld would not hold due to the deterioration of the heater in the oxygen sputtering environment. At the elevated temperatures strip heater life was limited. The correlation between heater temperature and sapphire substrate temperature was established by measuring the change in length of a c-axis oriented sapphire substrate for a given heater temperature. The substrate temperature was then inferred from values of the linear expansion for sapphire perpendicular to the c-axis. More details of this calibration are presented in Appendix I.

A movable shutter was provided between the substrate and the target. The target was sputtered clean for about 10 minutes with the shutter closed. Then, without interrupting the sputtering process, the shutter was opened and deposition began. The sputtering gas was admitted to the chamber through a precision micrometer valve. Since the system was continuously pumped during deposition, a throttling valve was necessary to keep from overloading the diffusion pump. The inlet and exhaust valves were adjusted to provide a chamber pressure of 15×10^{-3} torr and a diffusion pump foreline pressure of 25×10^{-3} torr. Rated pumping speeds for the diffusion pump at this foreline pressure is about 250 liters per minute. The volume of the sputtering chamber is about 25 liters, so that the sputtering atmosphere was being completely renewed about 10 times per minute.

The sapphire substrates were prepared as discussed in Section 2.1. Epitaxy has been achieved at substrate temperatures as low as 700°C. Also epitaxial rutile films were formed at a variety of substrate temperatures up to 1200°C. At the upper heater temperature, heater life was so severely limited that further increase in substrate temperature was impractical. The deposition rate was approximately 25 Å/min for a power input density of 1.4 watts/cm^2 to the titanium target.

5.2 Structural Characterization

The film structure and epitaxial relationship was arrived at by reflection electron diffraction and x-ray diffraction data. Figure 22a shows the expected reflection electron diffraction pattern with the electron beam directed along [010] zone axis if the rutile film grows with its c-axis normal to the film plane. The diffraction pattern obtained for an epitaxial film grown on a (001) oriented rutile substrate is shown in Fig. 22b.

X-ray diffractometer traces of TiO_2 films grown on $(1\bar{1}02)$ oriented sapphire substrates show a single diffraction peak correspondong to a "d" spacing of 2.489Å. This can be interpreted as (101) rutile planes growing parallel to the substrate. In order to analyze the reflection electron diffraction data, diffraction patterns were calculated for the electron beam directed along the [101] and [010] directions with (101) planes parallel to the surface (see Fig. 23). This can be readily identified with the experimentally obtained diffraction patterns shown in Fig. 24. The angular rotation of the electron beam required to observe the [010] and [101] patterns is 90° and each individual pattern repeats with a period of 180° as expected for a tetragonal structure.

The data for rutile films grown on (0001) sapphire substrates is somewhat more ambiguous to interpret. X-ray diffractometer data indicate that (100) planes of rutile grow parallel to the (0001) planes of sapphire. Figure 25 shows reflection electron diffraction data which can be correlated with [010] and [001] directions of rutile. The calculated diffraction patterns are illustrated in Fig. 26. Although there is apparent agreement between the measured and calculated results, an examination of the angular dependence of the diffraction patterns reveals that the repeat period

FIG. 22

CALCULATED AND EXPERIMENTAL RED PATTERN FOR RUTILE

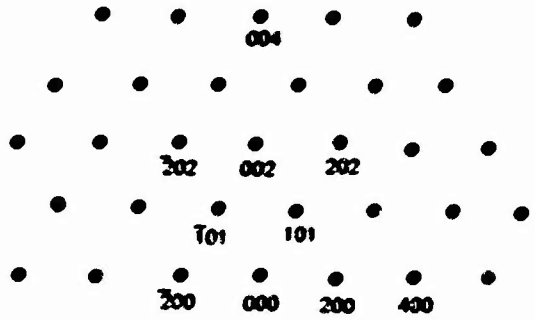

a) CALCULATED RED PATTERN FOR [010] DIRECTION OF RUTILE WITH (001) PLANES PARALLEL TO FILM SURFACE

b) RED OF TiO_2 ON [001] RUTILE

FIG. 23

CALCULATED RED PATTERNS FOR RUTILE FILM WITH (101) PLANES PARALLEL TO SURFACE

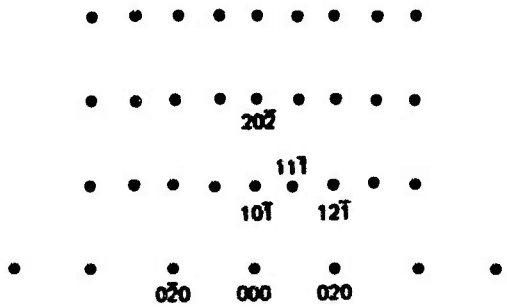

ELECTRON BEAM DIRECTED ALONG [101]

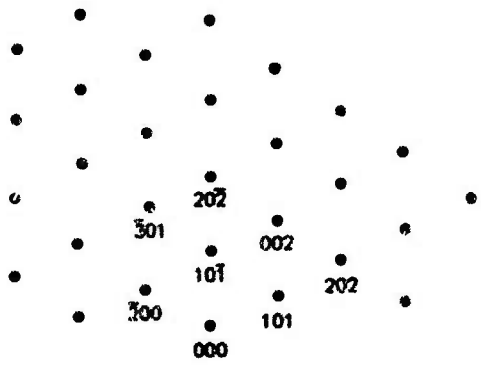

ELECTRON BEAM DIRECTED ALONG [010]

FIG. 24

RED OF TiO_2 ON (1102) Al_2O_3

[101]

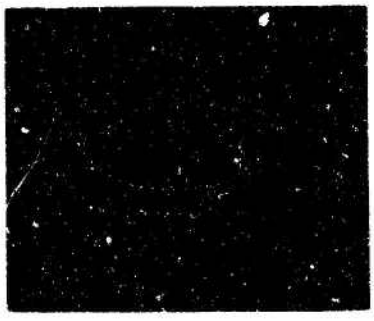

[010]

FIG. 25

RED OF TiO_2, ON (0001) Al_2O_3

[010]

[001]

FIG. 26

CALCULATED RED PATTERN FOR TiO_2 FILM WITH (001) PLANES PARALLEL TO SURFACE

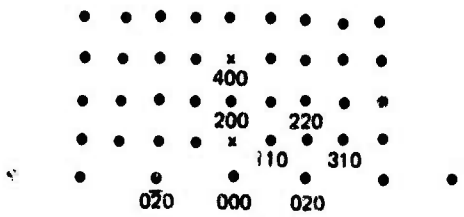

ELECTRON BEAM IN [001] DIRECTION

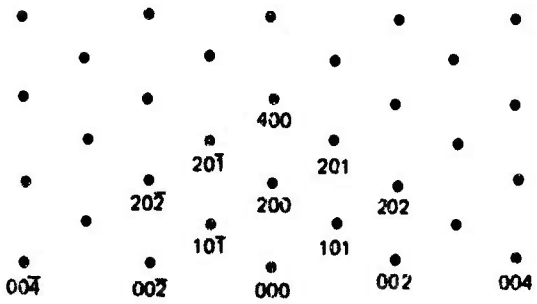

ELECTRON BEAM IN [010] DIRECTION

for the [010] and [001] patterns is 60° rather than 180°. In addition the two patterns alternate with a 30° period rather than 90°. This symmetry cannot be explained on the basis of the tetragonal symmetry of rutile. There is no evidence in the literature that a hexagonal modification of TiO_2 exists. A careful examination of the diffraction patterns reveals that the higher order reciprocal lattice points occur in pairs. A similar effect is observed in the diffraction data for chemical vapor deposited films on (0001) sapphire presented by Goshtogore and Norieka (Ref. 13). Furthermore, (100) rutile planes are identified as growing parallel to (0001) sapphire planes. However, a point of confusion arises with their assessment of the epitaxial relationship between the film and substrate. The reciprocal lattice vectors [001] and [011] of rutile are identified with the [110] direction of sapphire. This appears to be in error and a further comparison of results becomes impossible.

A tentative interpretation of our observations is the following. The (0001) plane of sapphire exhibits bi-3-fold symmetry. The atomic arrangement of sapphire in this plane cannot accommodate, in an unambiguous fashion, the atom arrangement of (100) planes of rutile which have two fold symmetry. A reasonable speculation is that three equivalent nucleation sites may occur on the (0001) sapphire which would give rise to an unusual twinned cyrstal arrangement exhibiting the six-fold symmetry observed. Thicker films are being grown which will give unambiguous back reflection data required to resolve this issue. Electron micrographs of replicated surfaces of rutile films grown on (0001) and ($1\bar{1}02$) sapphire (see Figs. 27 and 28) show that the films grown on the (0001) substrates are considerably rougher than those grown on ($1\bar{1}02$) substrates. This rough topography may be indicative of highly twinned growth on (0001) substrates.

5.3 Future Work

Optical waveguiding experiments will be carried out with rutile films grown on ($1\bar{1}02$) sapphire. Deposition parameters will be optimized to yield films with the best optical quality. Optical and electrical properties of the film will be fully characterized. Epitaxy of rutile on lithium niobate substrates will be explored.

FIG. 27

ELECTRON MICROGRAPH OF TiO_2 ON (0001) Al_2O_3

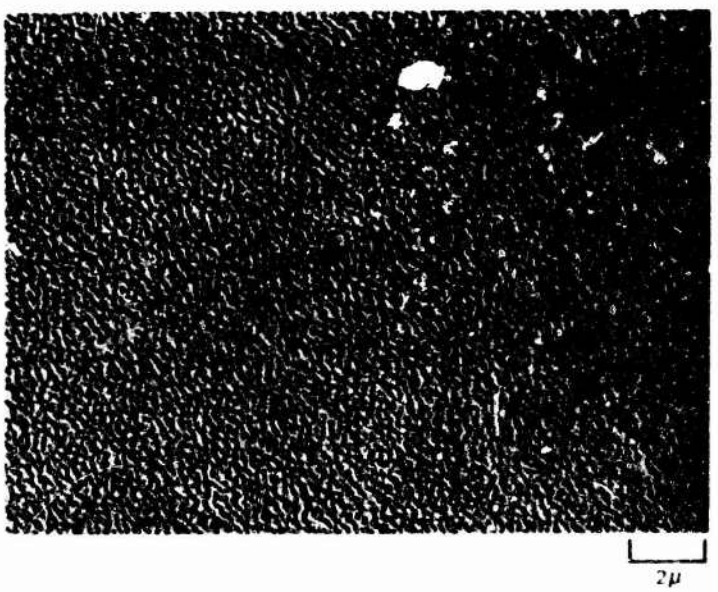

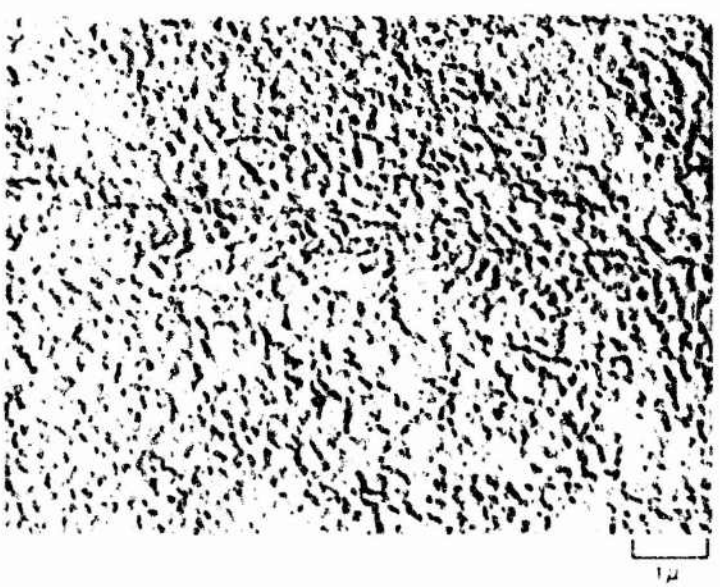

FIG. 28

ELECTRON MICROGRAPH OF TiO_2 ($1\bar{1}02$) Al_2O_3

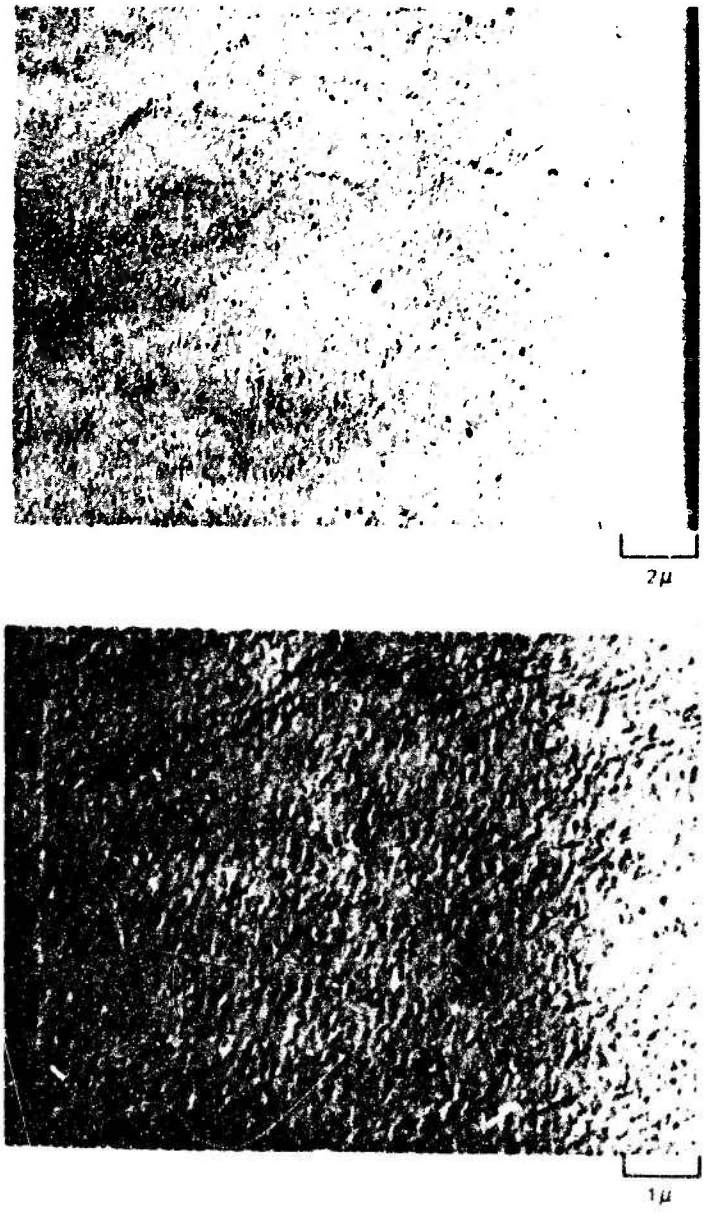

6.0 REFERENCES

1. H. M. Manasevit, F. M. Erdmann and W. I. Simpson, J. Electrochem. Soc., 118 1864 (1971).

2. Y. M. Yim, E. J. Stofko, P. J. Zanucchi, J. I. Pankove, M. Ettenburg and S. L. Gilbert, J. Appl. Phys., 44, 292 (1972).

3. P. J. Hagon and L. Dyal, Proc. 1972 Ultrasonics Symposium, p. 274 (1972).

4. J. H. Collins, P. J. Hagon and G. R. Pulliam, Ultrasonics, 8, 218 (1970).

5. G. Galli and J. E. Coker, Appl. Phys. Letters, 16, 439 (1970).

6. J. A. Rozgonyi and W. J. Polito, J. Vac. Sci. Technol., 6, 115 (1969).

7. T. C. Lim, E. A. Kraut and B. R. Titman, Appl. Phys. Letters, 17, 34 (1970).

8. T. Inoue and M. Ohyama, Solid State Communications, 8, 1309 (1970).

9. C. S. Fuller, K. B. Wolfstirn and H. W. Allison, Appl. Phys. Letters, 4, 48 (1964).

10. C. S. Fuller and J. M. Whelan, J. Phys. and Chem. of Solids, 6, 173 (1958).

11. L. J. Vieland, J. Appl. Phys., 33, 2007 (1962).

12. S. Zerfoss, R. G. Stokes and C. H. Moore, J. Chem. Phys., 16, 1166 (1948).

13. R. N. Goshtogore and A. J. Norieka, J. Electrochem. Soc., 117, 1310 (1970).

APPENDIX I

SUBSTRATE TEMPERATURE MEASUREMENT

One of the more difficult pieces of data for the experimenter in thin film vacuum deposition to obtain is substrate temperature during film growth. A common situation is found where a film is to be grown on one side of a planar substrate. The substrate surface must be exposed to the deposition source; therefore, the heating of the substrate must be arranged so as not to interfere with the line of right path of the deposit. Systems utilizing radiation exclusively for heating and temperature monitoring must operate in the region where the substrate is strongly absorbent. For sapphire this would require optics and energy source operating above 7μ wavelength.

The most common method of substrate heating is to place the substrate in contact with a solid heat source at the temperature desired. Various methods are used to insure that the substrate is at the same temperature as the source. Substrates can be held to the heater by gravity, mechanically clamped, or bonded with some good heat transfer medium. The most satisfactory method to ensure that the substrate follows the heater temperature is through the use of a bonding material. However, this method suffers from the fact that almost any bonding material will have an appreciable vapor pressure at elevated temperature thereby constituting a serious source of contamination.

Through a series of experiments which involved the normal operations of loading the substrate in the sputtering system and pumping down, we have found that a substrate simply held by gravity on a heater, while not necessarily achieving the same temperature as the heater, will repeatedly come up to very nearly the same equilibrium temperature. The correlation between heater temperature and sapphire substrate temperature was then established by measuring the change in length of a c-axis oriented sapphire substrate for a given heater temperature. The substrate temperature was then inferred from values of the thermal linear expansion for sapphire perpendicular to the c-axis.

The heater was a tantalum strip heater, identical to those used in the major portion of this program. The heater temperature was determined with an optical pyrometer at temperature above 800°C and with a chromel-alumel thermocouple spot welded to the heater strip at temperatures below 800°C. At 800°C, agreement between the two was within 5°.

The length measurements were made with a cathotometer capable of reading to 0.001 cm. Observed changes in sapphire length ranged from about 0.010 cm at 250°C substrate temperature to 0.094 at 1400°C substrate temperature. Observations were made for gas pressures of less than 2×10^{-3} torr, 10^{-2} and 10^{-1} torr. The thermal

expansion data for c-axis oriented sapphire used for this study are presented in Fig. A1. The calibration curves resulting from these measurements are shown in Fig. A2. All curves lag the heater temperature considerably at the lower temperatures but rapidly approach it for heater temperature above 1000°C. As expected the low temperature lag is most pronounced for low gas pressures. The low temperature lag is least for the case where a thin Al_2O_3 slide is used as a liner. This is indeed fortunate since this liner is used primarily to reduce substrate contamination from the heater. At higher temperatures, however, the liner appears to cause a slight reduction of substrate temperature as opposed to the bare heater.

ELONGATION OF SAPPHIRE VS TEMPERATURE

⊥ TO C AXIS

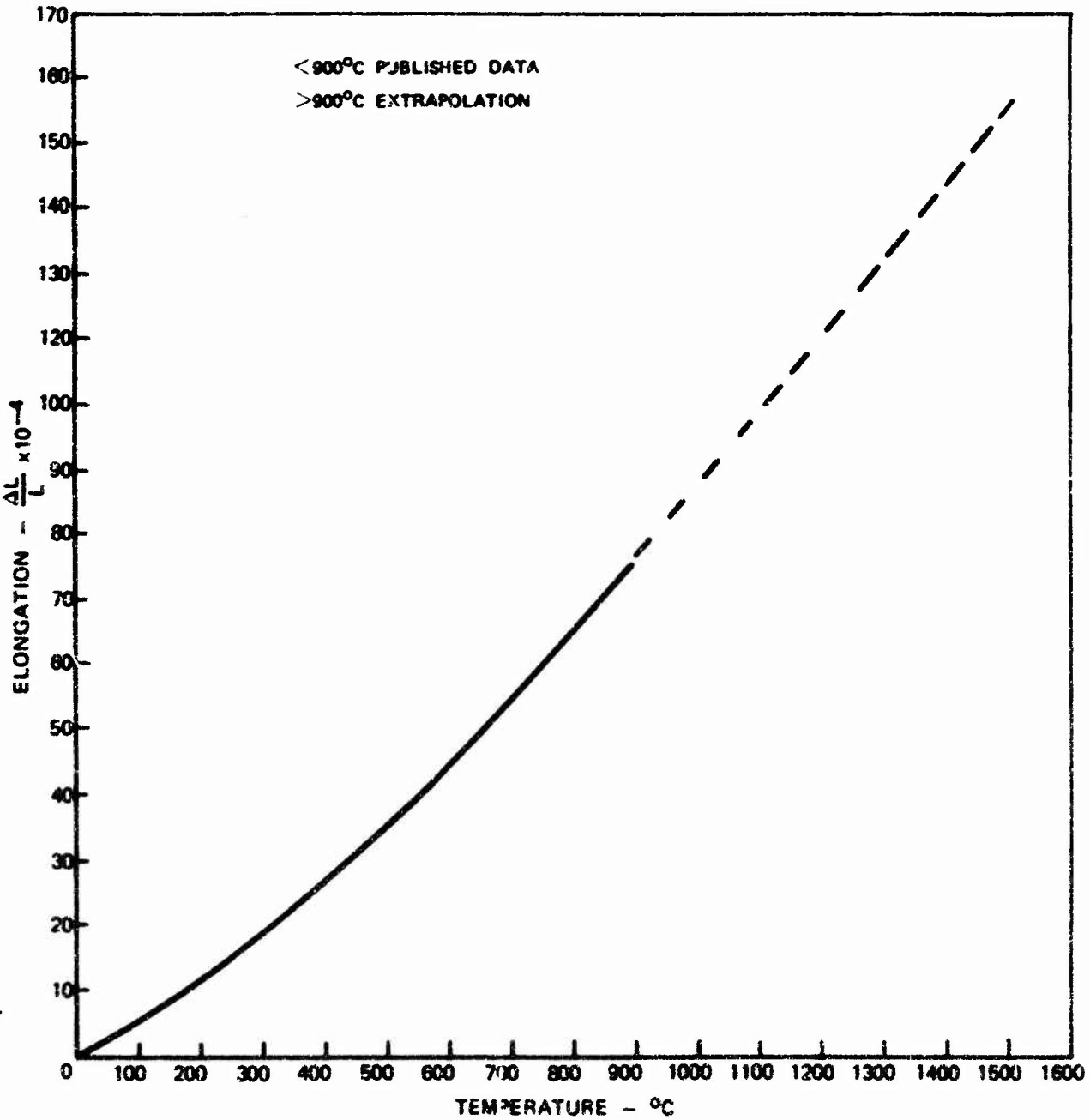

FIG. A2

TANTALUM HEATER TEMPERATURE VS SAPPHIRE SUBSTRATE TEMPERATURE

	O	< 2 M TORR	N_2
	X	10 M TORR	N_2
WITH Al_2O_3 SLIDE	Δ	10 M TORR	N_2
	□	100 M TORR	N_2